The EMBO Journal vol.10 no.9 pp.2353 - 2361, 1991

Chromophore motion during the bacteriorhodopsin photocycle: polarized absorption spectroscopy of bacteriorhodopsin and its M-state in bacteriorhodopsin crystals

Gebhard F.X.Schertler[1], Richard Lozier[2], Hartmut Michel[3] and Dieter Oesterhelt

Max-Planck-Institut für Biochemie, D-8033 Martinsried, FRG

[1]Present address: MRC Laboratory of Molecular Biology, Hills Road, Cambridge CB2 2QH, UK

[2]Present address: Laboratory of Chemical Physics, NIH, Bethesda, MD 20205, USA

[3]Present address: Max-Planck-Institute für Biophysik, Heinrich-Hoffmann-Strasse 7, D-6000 Frankfurt/M 71, FRG

Communicated by R.Henderson

The three-dimensional crystallization of bacteriorhodopsin was systematically investigated and the needle-shaped crystal form analysed. In these crystals the M-intermediate forms 10 times faster and decays 15 times more slowly than in purple membranes. Polarized absorption spectra of the crystals were measured in the dark and light adapted states. A slight decrease in the angle between the transition moment and the membrane plane was detected during dark adaptation. The crystallization of a mutated bacteriorhodopsin, in which the aspartic acid at residue 96 was replaced by asparagine, provided crystals with a long lived M-intermediate. This allowed polarized absorption measurements of the M-chromophore. The change in the polarization ratio upon formation of the M-intermediate indicates an increase in the angle between the main transition dipole and the membrane plane by 2.2° ± 0.5, corresponding to a 0.5 Å displacement of one end of the chromophore out of the membrane plane of the bacteriorhodopsin molecule.

Key words: absorption spectra/bacteriorhodopsin/chromophore/crystallization/*Halobacterium*

Introduction

Bacteriorhodopsin is part of an efficient light energy transducing system in *Halobacterium halobium* (Oesterhelt and Tittor, 1989). The retinal proteins sensory rhodopsin I and pigment P_{480} (phoborhodopsin, sensory rhodopsin II) function as light sensors. The light energy is transformed into electrochemical energy by the chloride pump halorhodopsin (HR) and the proton pump bacteriorhodopsin (BR). Several ion transport systems are involved in storing the captured light energy in a potassium gradient for dark periods (Wagner *et al.*, 1978).

The structure of bacteriorhodopsin has been solved to 2.8 Å in projection (Baldwin *et al.*, 1988) and to lower resolution in three dimensions (Tsygannik and Baldwin, 1987) by low dose electron diffraction and imaging. Recently an atomic model has been proposed based on the improved resolution of the latest electron density map (Henderson *et al.*, 1990). It confirmed the presence of seven hydrophobic transmembrane α-helical segments in the polypeptide chain (Ovchinnikov *et al.*, 1979) and the assignment of the sequence to the structure (Engelman *et al.*, 1980; Popot *et al.*, 1989).

Neutron diffraction has determined the position in projection of the retinal (Jubb *et al.*, 1984; Heyn *et al.*, 1988). The all-*trans* polyene chain of the retinylidene moiety is tilted by 20° to the membrane plane (Heyn *et al.*, 1977) and the polyene plane is oriented perpendicularly to the membrane plane (Earnest *et al.*, 1986). Resonance Raman and FTIR studies (reviewed in Stockburger *et al.*, 1986; Mathies *et al.*, 1991; Siebert, 1991) have detailed the conformation and configuration of retinal in the protein binding pocket. Incorporated into the structural model (Henderson *et al.*, 1990) the interaction with several tryptophan residues becomes obvious; the position of these tryptophans was directly derived from the electron density map.

Fluorescence energy transfer measurements and site directed mutagenesis had already some time ago implicated several tryptophan and tyrosine residues in the formation of a retinylidene binding pocket (Polland *et al.*, 1986a; Khorana, 1988; Rothschild *et al.*, 1989). Among other residues of apparent functional importance two aspartic acids in positions 85 and 96 are below and above the Schiff base of retinal in the structural model and dominate two half channels formed by helices B, C, F and G. Replacement of Asp85, Asp96 and Asp212 with asparagine indeed abolishes proton pumping substantially, strongly suggesting their involvement in proton transport (Mogi *et al.*, 1988; Butt *et al.*, 1989; Gerwert *et al.*, 1989).

Optical spectroscopy demonstrated that the retinylidene chromophore is photo-isomerized in the primary reaction and that a sequence of dark reactions in BR and HR couples ion translocation to the regeneration of the initial state.

The intermediates, with life-times between the femto- and the millisecond range, of this photocycle in bacteriorhodopsin have been designated J, K, L, M, N and O in the order of their appearance in the cycle after the light induced isomerization. The key events that link the cycle to ion translocation are the isomerization of the 13-*cis* chromophore in the photoreaction, the deprotonation of the 13-*cis* retinylidene Schiff base and its reprotonation during the decay of the M-intermediate.

Similar ion translocation mechanisms for HR and BR both involving the retinal chromophore isomerization and ion binding to charged amino acid side chains in the transmembrane segment have been proposed, although in HR the chromophore Schiff base does not become deprotonated during ion translocation (Oesterhelt *et al.*, 1986; Hegemann *et al.*, 1987; Oesterhelt and Tittor, 1989).

In all models proposed to explain the mechanism of the two ion pumps, however, the isomerization of the chromophore plays a central role (Fang *et al.*, 1983; Kölling

et al., 1984; Trissl and Gärtner, 1987; Fodor *et al.*, 1988a,b; Rothschild *et al.*, 1989; Henderson *et al.*, 1990). Measurements of the orientation of the chromophore in intermediate states during the photocycle may therefore help to provide further arguments to discriminate between different models.

Bacteriorhodopsin crystallizes in a pseudohexagonal needle-shaped crystal form (Michel and Oesterhelt, 1980; Michel, 1982). These crystals are optically uniaxial (i.e. the extinction coefficient perpendicular to the optical axis c has the same value in all directions) which allows straightforward calculation of the angle between the transition moment and the c-axis of the crystal (equations 2 and 3).

To obtain this information on the orientation of the retinylidene chromophore, polarized absorption measurements were carried out on light adapted and dark adapted bacteriorhodopsin crystals. The packing of the molecules in these crystals is known (Michel, 1982). This allows a correlation of the results obtained on the crystals with data obtained from purple membrane.

Replacement of Asp96 in bacteriorhodopsin by Asn leads to a retardation of the M-intermediate decay and enabled us to measure the orientation of the retinylidene chromophore in the M-state at room temperature. The methods described here may be applied in the future to obtain information on other intermediates at lower temperatures.

Results

Crystallization

The crystallization of bacteriorhodopsin in the form of hexagonal rods (form A; Michel and Oesterhelt, 1980; Michel, 1982) was improved by the variation of several parameters. First, instead of dissolving purple membranes in *n*-octyl-β-D-glucopyranoside (OG) by stirring the sample for 3 days at 34°C, dissolution in Triton X-100 at 34°C overnight reduced the amount of denatured material after solubilization. The detergent exchange by chromatography on DEAE–Sephacel led to a preparation with better crystallization properties. With such samples less denatured material was produced during crystallization. Prevention of denaturation during crystallization was important for reduction of the number of crystal nucleation sites. This allowed the growth of bigger and slightly better ordered crystals. The number of crystals with flat hexagonal cross sections which are best suited for spectroscopic experiments was enhanced.

The reproducibility of crystal preparation was further improved by replacement of heptane-1,2,3-triol as an amphiphilic small molecule by a mixture of benzamidine hydrochloride and D,L-pipecolinic acid. This latter compound acts as a stabilizing agent during crystallization. It increases the solubility of bacteriorhodopsin and shifts the phase separation between aqueous phase and detergent phase to higher salt concentrations. Benzamidine, on the other hand, reduces the solubility of bacteriorhodopsin considerably and therefore compensates for the opposite effect of D,L-pipecolinic acid. In addition, it also shifts the phase separation to higher ionic strength and thus separates very well the region of crystallization from that of phase separation. A comparison of the influence of different additives on the crystallization of bacteriorhodopsin is given in Scheme 1.

As precipitating agent in the mother liquid, a mixture of ammonium sulphate and sodium phosphate pH 5.6 instead of ammonium sulphate alone was found to be optimal. Ammonium sulphate alone destabilized solubilized bacteriorhodopsin slightly and led to increased amounts of denatured material in the crystallization droplets. In addition a competing aggregation process, i.e. the formation of bacteriorhodopsin containing fibres, was favoured by ammonium sulphate. If crystals were resuspended in detergent solutions without additives, conversion to fibrous material took place within a few days.

Sodium phosphate was found to stabilize solubilized bacteriorhodopsin and in the presence of benzamidine and D,L-pipecolinic acid no fibre formation was observed. A disadvantage of using sodium phosphate as the precipitating agent was that it is a stronger precipitant, resulting in an increased nucleation rate. The higher number of nucleation events limited the ultimate crystal size. By combining ammonium sulphate with sodium phosphate, reasonable nucleation kinetics were achieved and the tendency to form fibres was suppressed.

In addition to bacteriorhodopsin crystals prepared from purple membranes of *H.halobium* strain S9, bacteriorhodopsin from mutant strain 326 of *Halobacterium* sp. GRB (Soppa and Oesterhelt, 1989) was crystallized. This mutant protein carrying an asparagine in position 96 of the polypeptide chain instead of aspartic acid (BR D96N, Soppa *et al.*, 1989) has a slower photocycle than the wild type bacteriorhodopsin due to a slower decay time of ~500 ms at room temperature in the purple membrane (Butt *et al.*, 1989; Miller and Oesterhelt, 1990). Therefore it could conveniently be used to record spectra of the M-intermediate in crystals. Since bacteriorhodopsin from *Halobacterium* sp. GRB has an amino acid sequence identical to that from *H.halobium*, crystal spectra are also expected to be identical. The crystallization of the mutant bacteriorhodopsin had to be carried out in the presence of 2% benzamidine and only phosphate as precipitating agent because the stability was reduced. Therefore, crystallization was speeded up by using benzamidine to reduce the solubility and increase the probability of nucleation. Sodium phosphate was used to increase the rate of precipitation. With this method small crystals suitable for spectroscopic experiments could be obtained within 2 days.

Photochemical activity of bacteriorhodopsin in the crystallized state

The formation and the decay of the M-intermediate were measured with a microspectrophotometer that was optically coupled to a dye laser which produced light pulses of 20 ns at 480 nm. The signals from the photomultiplier of the microspectrophotometer were recorded with a digital oscilloscope. This arrangement is suitable for flash photolytic experiments on single protein crystals. The result of a typical flash experiment is shown in Figure 1. It demonstrates photoactivity of bacteriorhodopsin molecules in the crystal and the interesting fact of M-intermediate formation and decay with kinetics different from that of bacteriorhodopsin in purple membrane or of detergent solubilized bacteriorhodopsin. The rise time of M is similar to solubilized BR in 500 mM phosphate and 1% OG at pH 5.6 ($t_{½}$ = 6 μs) and is about eight times faster than in purple membranes. The decay of M on the other hand is 15–20 times slower than in the purple membrane ($t_{½}$ 150 ms). The half-time of

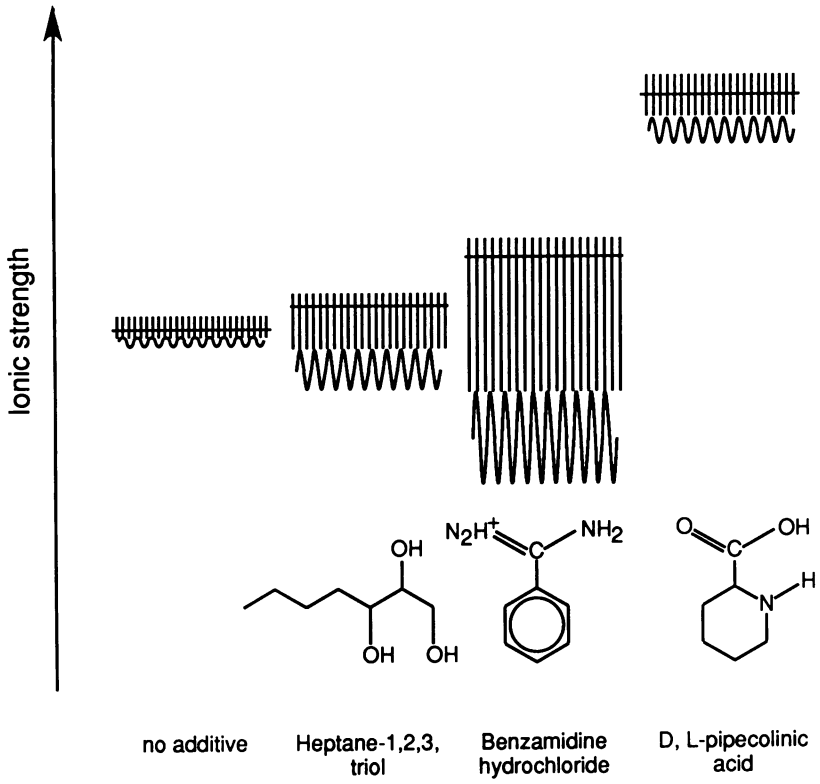

Scheme 1. The influence of additives on phase separation and crystallization. The horizontal line marks the ionic strength at which phase separation occurs. The zones hatched with vertical lines symbolize the region of fast crystallization because of a high nucleation probability. As a result only many small crystals are formed. The wavy line demarcates the zone of low nucleation probability and best crystallization. Only in this zone are large and well ordered crystals formed. The first lane shows that the crystallization zone of detergent solubilized bacteriorhodopsin without any additive is narrow and phase separation and crystallization coincide. The presence of the additive heptane triol shifts the phase separation to higher ionic strength and reduces the solubility of the protein–detergent complex, thus the zone of optimal crystallization is enlarged and shifted to lower ionic strength. At concentrations >1% the positive effect of heptane triol is obscured by its destabilizing effect on bacteriorhodopsin. The addition of benzamidine to the crystallization mixture results in an even stronger separation of the zone of best crystallization from the phase separation. It reduces the solubility of the protein–detergent complex and stabilizes bacteriorhodopsin. The addition of D,L-pipecolinic acid results in a remarkable stabilization of bacteriorhodopsin. Its presence shifts the phase separation to higher ionic strength and it increases the solubility of the protein–detergent complex. Similar influences of these additives could be observed for a range of detergents in which crystallization of bacteriorhodopsin was successful. The general features of the scheme hold for octylglucoside thiooctylglucoside, thioheptylglucoside and octyl-dihydroxi-propyl-sulfoxide.

decay of M in solubilized BR was 4.5 ms, similar to purple membranes. The measured half-times of decay in the crystals varied maximally by a factor of five depending on parameters such as crystallization additives, precipitant, measuring buffer, pH and ions present.

Polarized absorption spectra

Polarized absorption spectra were recorded on a microspectrophotometer equipped for actinic illumination to produce the M-intermediate. Hexagonally shaped needles are optically uniaxial and their angular dependence of the absorption at a given wavelength is described by equation (1) (Eaton and Hofrichter, 1981).

$$OD(\Theta) = \log (I_o/I_\theta) = -\log(10^{-ODa}\sin^2\Theta + 10^{-ODc}\cos^2\Theta) \quad (1)$$

I_o is the incident intensity and I_θ is the transmitted intensity for the electric vector of the plane-polarized light forming an angle Θ with the long needle axis c. ODc and ODa are the optical densities measured with the plane of polarization being parallel to the axis c and the axis a (normal to axis c), respectively.

The measuring area of the photometer was aligned to coincide exactly with the rotation axis of the specimen table of the instrument. A crystal was placed in the rotation axis. Spectra were taken for a series of angles between the plane of polarization of the measuring light beam and the long crystal axis (c-axis) by rotating the crystal around the optical axis of the instrument. Figure 2 shows the angular dependence of absorption for BR_{570} and the M-state. The curves shown in Figure 3 are calculated according to equation (1). The calculated angular dependence of absorption at the maximum of the retinal absorption fit the experimental data not only in the case of the initial state BR_{570} but also for the spectra of the M-intermediate. This is a good test for the performance of the microspectrophotometer arrangement under actinic illumination of the crystal, i.e. no artifactual depolarization effects occur.

In principle, a perfect crystal should have no background absorption due to intrinsic absorption or light scattering except for the absorption due to the chromophore. In practice, however, this may not be true. Examination of the data in Figure 2 shows an obvious background. In Figure 2A for example it is clear that the absorption of BR_{570} changes by more than a factor of 10 with polarizer parallel or perpendicular to the needle axis. Assuming the same ratio for residual BR_{570} in the spectrum of the M-intermediate of Figure 2B, a clear background level can be deduced. This could be due, for example, to light scattering by microscopic imperfections in the crystals. Some of the residual absorption

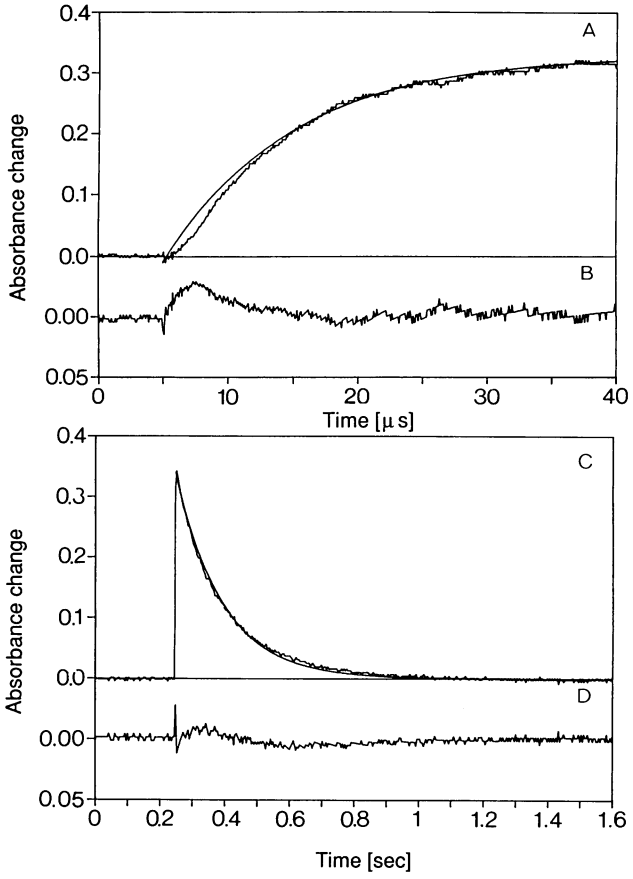

Fig. 1. Kinetics of M formation and M decay in a single BR crystal. Crystals from bacteriorhodopsin of *H.halobium* S9 were grown and mounted in a buffer containing 2.6 M sodium phosphate pH 5.6, 1% β-D-octylglucoside, 1% benzamidine, 1% D,L-pipecolinic acid. The absorption change after a 20 ns laser flash at 480 nm was recorded at two different time scales to observe the rise (**A**) and decay (**C**) of the M-intermediate at 410 nm. A single exponential rise or decay was drawn over the measuring trace. The lower curves (**B** and **D**) are the residual differences between the exponential function and the measured values. The production of M ($t_{½}$ = 8 μs) after a flash is about eight times faster than in purple membrane. The non-exponential rise indicates the presence of other photocycle intermediates in the crystal before the M-intermediate is formed. The decay of M ($t_{½}$ = 150 ms) is 15–20 times slower than in purple membrane.

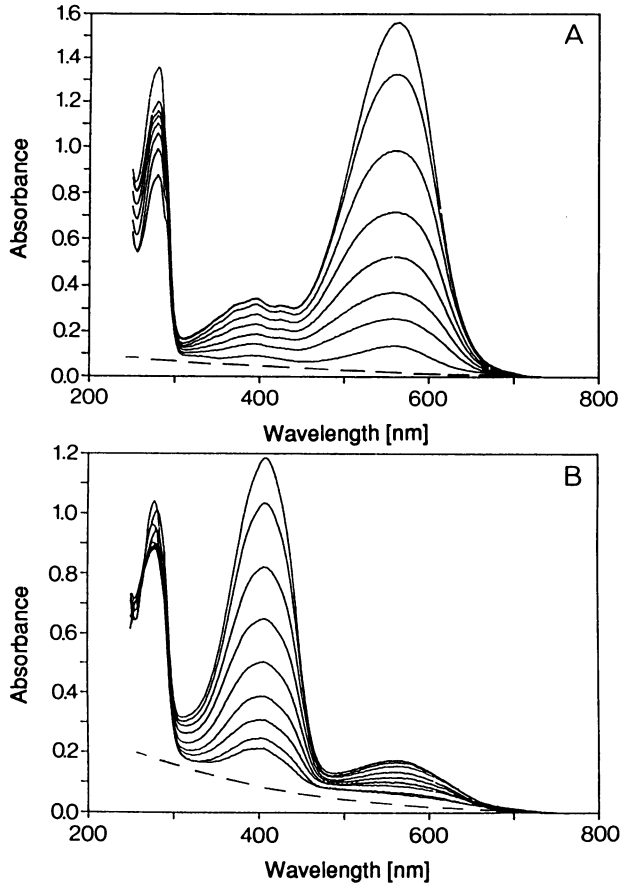

Fig. 2. Polarized absorption spectra of BR_{570} and the M_{410}-intermediate state in needle crystals of a mutated bacteriorhodopsin from *Halobacterium* sp. GRB strain 326 (Asp96 → Asn). Crystals of bacteriorhodopsin from the mutant strain 326 were grown as described. The crystals were mounted in a buffer containing 2.6 M sodium phosphate pH 5.6, 1% β-D-octylglucoside, 1% benzamidine and 1% D,L-pipecolinic acid and light adapted before measurements were carried out. (**A**) Absorption spectra of the BR_{570} state at angles between 0 and 90° between the long needle axis and the plane of the linearly polarized measuring light were recorded in a microspectrophotometer. The applied background correction is shown below the spectra. (**B**) To enrich the M-intermediate in the photostationary equilibrium the crystals were continuously illuminated as described in Materials and methods. Polarized absorption spectra were recorded on exactly the same small area of the crystal (black spot in Figure 5) and with exactly the same setting of the instrument as for the measurements on BR_{570}. The applied background correction is shown below the spectra.

at 570 nm could also be due to the presence of another intermediate. The crystals are known to be somewhat mosaic (Michel, 1982) from X-ray diffraction experiments implying the presence of internal microscopic domain boundaries. Thus, the existence of background absorption due to light scattering is plausible. Furthermore, the apparent dichroic ratio also varies strongly with wavelength without background correction. For quantification of the background absorption we assumed a polarization ratio which is constant over the width of the absorption band. In spectra of the M-intermediate the residual polarized absorption of the molecules in the BR_{570} state could be used as additional information to determine the background absorption in the spectra and to make sure that the same corrections were applied to the spectra under illuminating and non-illuminating conditions. The final polarization ratios were the values averaged over the half-width of the main retinylidene absorption band.

The angles of transition moments relative to the c-axis were determined from the polarization ratio $P_{c/a}$ which is the ratio of ODc and ODa after background correction. The angle Φ defines the opening angle of a double cone formed by the transition moments of the chromophores around the long axis c of the crystal. Under the assumptions that retinal is a linear absorber, that the chromophores absorb light independently, and that the rod-shaped crystals are uniaxial, the following relation holds (Hofrichter and Eaton, 1976).

$$P_{c/a} = ODc/ODa = 3\epsilon\cos2(\Phi)cd \,/\, (3/2)\epsilon\sin2(\Phi)cd \quad (2)$$

Protein concentration c, extinction coefficient ϵ and crystal thickness d cancel. The chromophore angle Φ can be calculated directly from the measured polarization ratio $P_{a/c}$ according to equation (3).

$$\Phi = \arcsin \pm \sqrt{\left(\frac{2}{2 + P_{c/a}}\right)} \quad (3)$$

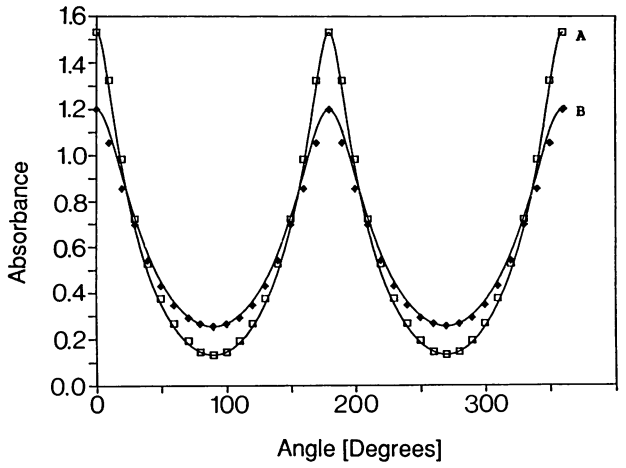

Fig. 3. Angular dependence of the absorption of BR_{570} at 570 nm and under actinic light conditions for the intermediate M-state at 408 nm in a BR crystal. (**A**) The curve A for light adapted BR_{570} was calculated using equation (1) and the absorption values obtained with the plane of the linear polarized measuring light either parallel (ODc,0°) or normal to the long needle axis (ODa,90°). The dependence of the absorption was measured for different angles between the long needle axes c and the polarization plane at the absorption maximum 565 nm and the obtained values were plotted (□). (**B**) The curve B for the intermediate M-state was calculated in the same way, but all experimental measurements were carried out under continuous actinic illumination at the absorption maximum of the M-intermediate in the crystal at 408 nm (◆). The good correspondence between measured values and calculated curves even under actinic illumination shows that no corrections for instrumental depolarization are necessary.

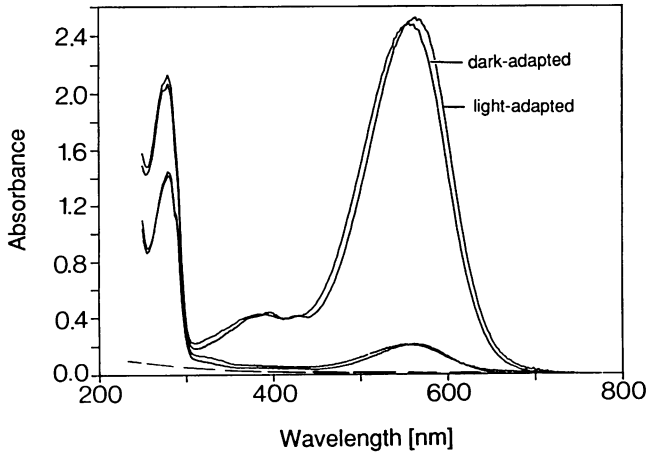

Fig. 4. Light adaptation of bacteriorhodopsin in hexagonally shaped crystals. Polarized absorption spectra parallel and perpendicular to the needle axis were recorded with minimal measuring light after a period of 2 h in the dark (**A**). After illumination of the crystal for 5 min, polarized spectra at 0 and 90° were measured on the light adapted crystals (**B**). The applied background correction is shown below the spectra.

Table I. Polarization ratios and chromophore angles

	$P_{c/a}$	Φ
H.halobium S9		
Dark adapted	13.2 ± 0.5	21.3° ± 0.4
Light adapted	12.6 ± 0.6	21.7° ± 0.5
Halobacterium sp. GRB BR-mutant Asp96 → Asn96		
M-state	11.0 ± 1.2	23.1° ± 1.1
BR_{570}-state (Light adapted)	13.7 ± 0.3	20.9° ± 0.2

Spectra of light and dark adapted crystals

Bacteriorhodopsin shows light−dark adaptation in the crystal similar to that in the solution used for crystallization. Figure 4 shows polarized absorption spectra of light and dark adapted BR crystals. The absorption values were corrected as described above. The polarization ratio $P_{c/a}$ and the corresponding chromophore angles were calculated and the values are summarized in Table I. We observed a small decrease in the angle of the transition moment of −0.4°. Because in dark adapted BR only half of the molecules are in the 13-*cis*, 15-*syn* form (Smith *et al.*, 1987) the angle of the transition moment is tilted by 0.8° towards the unique crystal axis during dark adaptation.

Spectra of the M-intermediate in the crystal

The kinetic experiment of Figure 1 showed that the rate limiting step of the photocycle is considerably slowed in the crystal. This allows an enrichment of the M-intermediate at room temperature upon continuous illumination. This was done with light from a xenon lamp fitted to the photometer. In fresh crystals of bacteriorhodopsin from strain *H.halobium* S9, the M-intermediate could not be enriched to >50% even with optimal illumination conditions. However, after a period of about 1 week in room light the same crystal allowed accumulation of >80% of the intermediate, apparently due to ageing of the crystal but otherwise for unknown reasons. Also, treatment of the crystals with buffer containing diethylether gave a similar result.

More elegantly, a point-mutated protein, BR D96N, with a slower photocycle was crystallized under slightly varied conditions and was used for this experiment. The mutant protein, BR D96N, had a half-time of decay of the M-intermediate of 3 s in the crystalline state.

This allowed accumulation of the M-intermediate to >80% in fresh and untreated crystals of BR D96N. Figure 5 shows crystals of the BR D96N. After illumination of part of the crystal with light above 550 nm this area turned yellow due to formation of the M-state. The black spot on the yellow part of the crystal is the area of the measuring beam of the microspectrophotometer. In Figure 2B a series of polarized absorption spectra of the illuminated crystal is shown.

After correction for the background as described above, the polarization ratios for the BR_{570} state and the M-intermediate in these crystals were determined and the corresponding chromophore angles were calculated. The values are listed in Table I. During the transition from BR_{570} to M the opening angle of the chromophore increased by 2.2°.

Discussion

In optical terms BR crystals represent a translucent but strongly anisotropic material that has some advantages over purple membrane suspensions and oriented films. Stray light problems are reduced allowing more accurate measurements in the UV (e.g. the region between 300 and 450 nm which contains some of the weak transitions of the chromophore is less disturbed by light scattering). The crystals are very well suited to measurements that require oriented samples because the protein is highly concentrated and the orientation

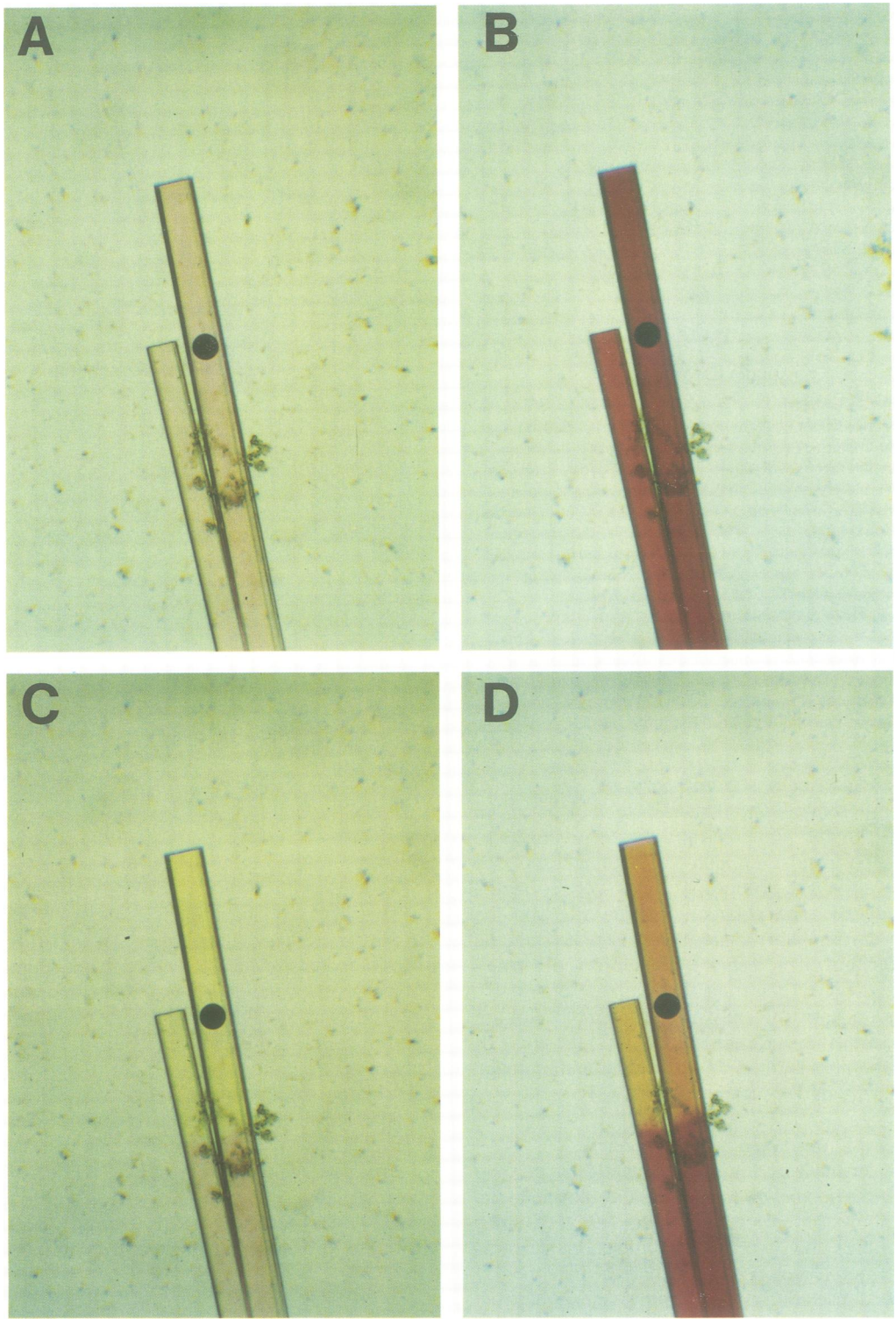

Fig. 5. Linear dichroism of BR_{570} and the M-intermediate state in bacteriorhodopsin crystals. Needle crystals of bacteriorhodopsin from *H.halobium* S9 were mounted in a buffer containing 2.6 M sodium phosphate pH 5.6, 1% β-D-octylglucoside, 1% benzamidine and 1% D,L-pipecolinic acid. The black spot on the crystal is the measuring area of the microspectrophotometer. (**A**) This picture of BR_{570} was taken with the polarization plane normal to the long needle axis (90°, normal c-axis). The absorption of the retinylidene moiety oriented in the crystal is minimal. (**B**) The polarization plane is parallel to the c-axis and maximal absorption of the BR_{570} state is observed. (**C**) This picture is taken while actinic light is continuously projected on one half of the crystals, enriching the M-intermediate state in the crystal. Because of its different absorption characteristics the illuminated half of the crystal turns yellow. The polarization plane is normal to the needle axis in this position and the absorbance of the M-intermediate state is minimal. (**D**) The picture is taken under the same continuous actinic light as in (C) but the polarization plane is parallel to the long crystal axis, and therefore the absorbance of M in the crystal is maximal.

is nearly perfect. Another important point is that the arrangement of the molecules in the sample is known (Michel, 1982) and the favourable symmetry of the crystals allows a straightforward interpretation of the results. However, the exact orientation of the molecule relative to the needle axis and the relationship between the needle axis

and the membrane plane could not be determined exactly.

The kinetic investigation of the crystalline material shows that the bacteriorhodopsin molecules in the crystals are photoactive. It is interesting to note that the M-intermediate is formed faster than in the purple membrane and decays more slowly. The values for the rise time and for the decay are strongly dependent on the crystallization and buffering conditions.

The faster rise of M in the crystals is similar to the fast rise times of M in the solubilized state. It is possible that the distances to groups which accept the proton from the Schiff base in solubilized bacteriorhodopsin is changed and that this effect is not reversed on crystallization, because the *n*-octyl-β-D-glucoside is not removed from the hydrophobic parts of the molecule during crystallization. About 30 *n*-octyl-β-D-glucoside molecules were found per bacteriorhodopsin molecule in the crystal (Michel, 1982).

A slower decay of M and lack of the O-intermediate is seen in the purple membrane at high pH and may be due to a decreased availability of protons to reprotonate the Schiff base. The slower decay of M in the crystalline form could be explained by a reduction of the availability of protons from the surface of the molecules in the crystal. On the other hand the decay of M is slow in spite of a low pH in the measuring buffer. Thus it seems more likely that a change in activation energies is responsible for the slow decay and would be revealed by a study of the temperature dependence of the kinetics.

Photo-stationary spectra of the M-state indicate an absorption maximum of the M-intermediate at 408 nm which is close to the 410 nm maximum of M in the membrane. The spectra show shoulders on the left and right sides of the M absorption band which could be due to stronger restriction of the rotation of the β-ionone ring around the 6,7-bond in the crystal similar to that observed at low temperatures. We conclude that the M-intermediate in the crystal is structurally similar to the M-intermediate in the membrane.

From the polarized absorption spectra and from the calculated polarization ratio the angle between transition moments and the long crystal axis was calculated. For these calculations we assume that we are dealing with a linear absorber (molecular extinction coefficients: $\epsilon z = 3\epsilon$; $\epsilon x = \epsilon y = 0$), which seems a good assumption for the extended retinylidene structure.

The second assumption made is that the crystals are uniaxial. Inspection of the X-ray diffraction pattern shows that along the 0,0,1 lattice line only every seventh reflection is present which can be interpreted as a 7-fold repeat along the long needle axis, probably a 7-fold screw axis. The crystal is built from aligned screws of bacteriorhodopsin molecules (Michel, 1982). Screws are optically uniaxial and the packing of parallel screws in a hexagonal crystal results in an optically uniaxial crystal. This was confirmed by rotation of a regular hexagonal crystal around the long needle axis. Identical absorption values were obtained each 60° which is not to be expected for a biaxial crystal.

The angle between the molecular axis of the retinylidene moiety and the purple membrane plane is $<27°$ (Korenstein and Hess, 1978) and most probably 20° (Heyn *et al.*, 1977). From the extended shape of the retinal in the protein and from the directions of the transition moments determined in thin all-*trans* retinal crystal plates (Drikos *et al.*, 1984) it is known that the main transition moment is nearly parallel to the molecular axis (which is defined as the straight line between atom 6 and the nitrogen of the Schiff base or the oxygen in the free retinal).

We conclude from our data that the bacteriorhodopsin molecules are arranged perpendicularly to the long needle axis with 21° between the main transition moment and the needle axis in light adapted crystals.

In the structural model of bacteriorhodopsin (Henderson *et al.*, 1990) the retinylidene Schiff base was positioned according to the present knowledge obtained by biophysical methods, especially resonance Raman and Fourier transformed infrared spectroscopy. The light adapted form of the chromophore is an all-*trans*, 15-*anti* configuration (Harbison *et al.*, 1986) and the cyclohexene ring linked to the polyene chain by a 6s-*trans* conformation (Harbison *et al.*, 1986; van der Steen *et al.*, 1986). The plane of the π-bond system is perpendicular to the plane of the purple membrane (Siebert *et al.*, 1991) with the methyl groups of the polyene chain pointing towards the cytoplasma. This fact was derived from linear dichroism measurement of purple membranes reconstituted with 3,4-dihydroretinal (Lin and Mathies, 1989). Scheme 2 shows the change in the chromophore

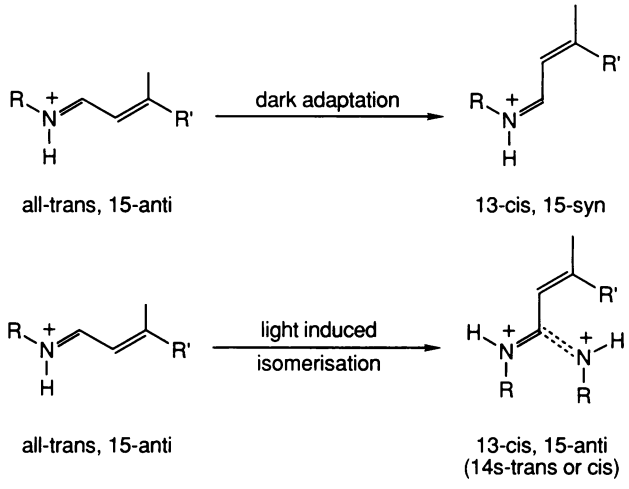

Scheme 2. Configurational and conformational change in the chromophore of bacteriorhodopsin. Only part of the retinal Schiff base is shown. R is lysin 216 and R′ is the rest of the retinal. The π-electron system of the retinylidene rest is perpendicular to the plane of the membrane and the methyl groups of the retinal point to the cytoplasmic surface of bacteriorhodopsin.

occurring during dark adaptation and after photo-isomerization initiating the catalytic cycle. Dark adaptation forms a 1:1 mixture of all-*trans*, 15-*anti* and a 15-*cis*, 15-*syn* chromophore (Smith *et al.*, 1987). Photo-isomerization of the all-*trans*, 15-*anti* Schiff base creates a 13-*cis*, 15-*anti* chromophore and it is still a matter of debate whether the 14,15 single bond changes its angle as well (Gerwert and Siebert, 1986; Fodor *et al.*, 1988b; Fahmy *et al.*, 1989). In Scheme 2 the two extreme positions i.e. 14s-*trans* and 14s-*cis* are both shown. The very short time observed for the formation of the J-intermediate of 450 fs (Dobler *et al.*, 1988) allows only a limited mass movement of about three methylene groups to create the 13-*cis* state. Whether there are additional movements of the chromophore later in the photocycle but before M-intermediate formation is not known. The dual double bond rotation during dark adaptation might be tolerated by the retinal binding pocket without drastic compensatory movement of the protein moiety i.e. amino acid side chain (R in Scheme 2). This would lead to

a more parallel arrangement of the transition moment of retinal and the plane of the membrane, as we observed experimentally. The photo-isomerization reaction in any case leads to a situation which requires a compensation of the protein moiety. Considering the tight packing of amino acid side chains around the retinal polyene chain and the cyclohexene ring by bulky tryptophan residues, it is plausible to assume that compensation occurs especially via the lysine 216 side chain (R in Scheme 2). This pull on the protein could explain both upward movement of retinal seen by the increase in the transition moment angle of the chromophore 2.2° and/or movement of helix G seen by time resolved X-ray analysis of purple membrane (Koch *et al.*, 1991). The maximum displacement calculated from the change in the transition moment is given by the sine of the change multiplied by the length of the retinal molecule, which is ~15 Å. This would be 0.57 Å. This value is large enough to be functionally relevant.

The photo-isomerization reaction requires compensatory rotation of the β-ϵ-methylene groups of Lys216 and leaves strain for the protein part independent of whether an additional rotation around the 14,15 single bond is assumed or not. A difference is found for the change in position of the Schiff base proton. Without rotation of the 14,15 bond the proton points to D96 after photo-isomerization while a 14,15 bond rotation allows the proton to keep its position on the side where D85 is positioned, but with some change in distance. Because the extracellular channel is the pathway of proton release and D85 the presumed proton acceptor, the latter position of the Schiff base after photo-isomerization seems more functionally relevant than a position where the proton faces the proton donating channel with D96 after photo-isomerization.

Materials and methods

Chemicals

The purity of detergents used was found to be crucial for the success of crystallization. For solubilization, Triton X-100 for scintillation techniques from Serva, Heidelberg, FRG, was used. The quality of *n*-octyl-β-D-glucopyranoside varied considerably even if obtained from the same supplier. Its purity was routinely checked by ^{3}H-NMR and GC-MS analysis after trimethylsilylation of the sugar hydroxyl groups. Larger amounts of these detergents were purchased only after several successful test crystallizations. D,L-pipecolinic acid was obtained from Aldrich. Benzamidine hydrochloride was obtained from Sigma; heptane-1,2,3-triol (high melting isomer) was obtained from Oxyl, Bobingen, FRG. Purple membrane was prepared according to Oesterhelt and Stoeckenius (1974).

Crystallization

Needle-shaped crystals of bacteriorhodopsin (BR) were prepared by a procedure similar to that introduced by Michel and Oesterhelt (1980) (see also Michel, 1982). Purple membrane suspension (4 ml, OD_{568} = 25) was added to 14 ml solubilization buffer (1% Triton X-100, 10 mM sodium phosphate pH 5.6) and the mixture stirred for 14 h at 34°C in the dark. The detergent was exchanged on a DEAE–Sephacel column (3 ml bed volume, 6 mm diameter) previously washed with 500 mM sodium phosphate pH 5.6 and equilibrated with solubilization buffer. After centrifugation at 100 000 *g* for 45 min at 20°C to remove residual membranes and denatured protein, the sample was loaded on to the ion exchange column. The column was slowly washed with 30 ml of exchange buffer (1% OG in 10 mM sodium phosphate pH 5.6) over a period of 3 h. Bacteriorhodopsin was eluted with high salt buffer (1% OG in 500 mM sodium phosphate pH 5.6) and the eluate fractionated to obtain the maximally concentrated BR solution. Further concentration to an OD_{552} of 30–50 was achieved with a Centricon 30 ultrafiltration device (Amicon). Benzamidine (1% w/v) and D,L-pipecolinic acid (1% w/v) were dissolved in the concentrated protein solution. Sodium phosphate solution (0.5 parts, 3 M, pH 5.6) and ammonium sulphate solution (0.5 parts, 4 M) were added to 1 part of the protein solution. This mixture was equilibrated over the vapour phase with a series of ammonium sulphate solutions (8 ml) in sealed plastic dishes (diameter 75 mm, height 30 mm), fitted with a plastic bench that has a depression which holds 50 μl protein solution. The concentrations of the bottom solution ranged from 2.4 to 3.1 M ammonium sulphate. Usually, a series with an increment of 0.05 M ammonium sulphate provided crystals of different sizes and shapes. From these, flat crystals, suitable for spectroscopic work, were selected.

The absorption spectra of crystals were measured in a buffer including detergent and additives (2.6 M sodium phosphate, pH 5.6, 1% OG, 1% benzamidine, 1% D,L-pipecolinic acid). Leaving out the additives leads to a transformation of the crystals to a filamentous material (Michel, 1982) within a few days.

Microspectroscopy

The crystals were mounted on a quartz microscope slide and were covered by a quartz cover slip that was fitted with small spacers of beeswax. The arrangement was sealed with a molten mixture of 1:1:1 lanolin, paraffin and paraffin oil.

Although most of the crystals appeared to be rods with a regular hexagonal cross section, some crystals growing on the surface of the protein solution had a flat hexagonal cross section. Such crystals are better suited for microspectrophotometric studies because a larger measuring area can be used and the optical path length is short enough to keep the absorption below 2.6. However, satisfactory spectra of smaller needles with regular cross section can also be obtained using a smaller measuring aperture. Polarized absorption spectra were measured with a Zeiss UMSP 80 microspectrophotometer equipped with an Ultrafluar 10× lens as objective and a second Ultrafluar 10× lens as condensor. The actinic light source for continuous illumination was a 75 W xenon lamp. The light was filtered through two heat protection filters and an OG 515 filter (2 mm) and focused on the crystal with a lens (f = 100 mm).

Kinetic measurements were performed on the same instrument. The slow amplifier of the photometer was disconnected and the photomultiplier signal was detected directly with a Tectronix 2430 digitizing oscilloscope. The actinic light source for flash photolysis experiments was an eximer laser EMG 53 MSC (Lambda Physics, Göttingen, FRG) that pumped a dye laser FL 3001 (Lambda Physics, Göttingen, FRG) with either Rhodamine 6B for excitation at 570 nm or Coumarin 120 for excitation at 480 nm. The laser beam was optically coupled to the microspectrophotometer with two mirrors and a focussing lens arranged so that the sample was hit by the light at an angle of 45° from the optical axis of the photometer.

Acknowledgements

We thank Susanne Meessen for preparing the purple membranes of the mutant strain 326. This work was supported by the Deutsche Forschungsgemeinschaft (SFB 143) and G.F.X.S. was holding a long term EMBO fellowship (ALTF 106-1988).

References

Baldwin,J.M., Henderson,R., Beckmann,E. and Zemlin,F. (1988) *J. Mol. Biol.*, **202**, 585–591.

Butt,H.J., Fendler,K., Bamberg,E., Tittor,J. and Oesterhelt,D. (1989) *EMBO J.*, **8**, 1657–1663.

Dobler,J., Zinth,W., Kaiser,W. and Oesterhelt,D. (1988) *Chem. Phys. Lett.*, **144**, 215–220.

Drikos,G. and Rüppel,H. (1984) *Photochem. Photobiol.*, **40**, 93–104.

Eaton,W.A. and Hofrichter,J. (1981) *Methods Enzymol.*, **76**, 175–261.

Earnest,T.N., Roepe,P., Braiman,M.S., Gillespie,J. and Rothschild,J. (1986) *Biochemistry*, **25**, 7793–7798.

Engelman,D.M., Henderson,R., McLachlan,A.D. and Wallace,B.A. (1980) *Proc. Natl Acad. Sci. USA*, **77**, 2023–2027.

Fahmy,K., Grossjean,F., Siebert,F. and Tavan,P. (1989) *J. Mol. Struct.*, **214**, 257–288.

Fang,J.M., Carriker,J.D., Balogh-Nair,Y. and Nakanishi,K. (1983) *J. Am. Chem. Soc.*, **105**, 5162–5164.

Fodor,S.P.A., Ames,B.A., Gebhard,R., van den Berg,E.M.M., Stoeckenius,W., Lugtenburg,J. and Mathies,R.A. (1988a) *Biochemistry*, **27**, 7097–7101.

Fodor,S.P.A., Pollard,W.T., Gebhard,R., van den Berg,E.M.M., Lugtenburg,J. and Mathies,R. (1988b) *Proc. Natl Acad. Sci. USA*, **85**, 2156–2160.

Gerwert,K. and Siebert,F. (1986) *EMBO J.*, **5**, 805–811.

Gerwert,K., Hess,B., Soppa,J. and Oesterhelt,D. (1989) *Proc. Natl Acad. Sci. USA*, **86**, 4943–4947.

Harbison,G.S., Smith,S.O., Pardoen,J.A., Courtin,J.M.L., Lugtenburg,J., Herzfeld,J., Mathies,R.A. and Griffin,R.G. (1986) *Biochemistry*, **24**, 6955–6962.
Hegemann,P., Tittor,J., Blanck,A. and Oesterhelt,D. (1987) In Ovchinnikov,Y. (ed.), *Retinal Proteins*. VNU Science Press, Utrecht, pp. 333–352.
Henderson,R., Baldwin,J.M., Ceska,T.A., Zemlin,F., Beckmann,E. and Downing,K.H. (1990) *J. Mol. Biol.*, **213**, 899–929.
Heyn,M.P., Cherry,R.J. and Müller,U. (1977) *J. Mol. Biol.*, **117**, 607–620.
Heyn,M.P., Westerhausen,J., Wallat,I. and Seiff,F. (1988) *Proc. Natl Acad. Sci. USA*, **85**, 2146–2150.
Hofrichter,J. and Eaton,W.A. (1976) *Annu. Rev. Biophys. Bioeng.*, **5**, 511–560.
Jubb,J.S., Worcester,D.L., Crespi,H.L. and Zaccai,G. (1984) *EMBO J.*, **3**, 1455–1461.
Khorana,H.G. (1988) *J. Biol. Chem.*, **263**, 7439–7442.
Koch,M.H.J., Dencher,N.A., Oesterhelt,D., Plöhn,H.J., Rapp,G. and Büldt,G. (1991) *EMBO J.*, **10**, 521–526.
Kölling,E., Gärtner,W., Oesterhelt,D. and Ernst,L. (1984) *Angew. Chem.* (Int. Ed. Engl.), **23**, 81–82.
Korenstein,R. and Hess,B. (1978) *FEBS Lett.*, **89**, 15–20.
Lin,S.W. and Mathies,R.A. (1989) *Biophys. J.*, **55**, 383a.
Mathies,R.A., Lin,S.W., Ames,J.B. and Pollard,W.T. (1991) *Annu. Rev. Biophys.*, in press.
Michel,H. (1982) *EMBO J.*, **10**, 1267–1271.
Michel,H. and Oesterhelt,D. (1980) *Proc. Natl Acad. Sci. USA*, **77**, 1283–1285.
Miller,A. and Oesterhelt,D. (1990) *Biochim. Biophys. Acta*, **1020**, 57–64.
Mogi,T., Stern,L.J., Marti,T., Chao,B.H. and Khorana,H.G. (1988) *Proc. Natl Acad. Sci. USA*, **85**, 4148–4152.
Oesterhelt,D. (1986) *Biophys. J.*, **49**, 651–662.
Oesterhelt,D. and Tittor,J. (1989) *Trends Biochem. Sci.*, **14**, 57–61.
Oesterhelt,D. and Stoeckenius,W. (1974) *Methods Enzymol.*, **31**, 667–678.
Oesterhelt,D., Hegemann,P., Tavan,P. and Schulten,K. (1986) *Eur. Biophys. J.*, **14**, 123–129.
Ovchinnikov,Y.A., Abdulaev,N.G., Feigina,M.Y., Kisleev,A.V. and Lobanov,N.A. (1979) *FEBS Lett.*, **100**, 219–224.
Polland,H.J., Franz,M.A., Zinth,W., Kaiser,W. and Oesterhelt,D. (1986a) *Biochim. Biophys. Acta*, **851**, 407–415.
Polland,H.J., Franz,M.A., Zinth,W., Kaiser,W., Kölling,E., Popot,J.L., Engelman,D.M., Gurel,O. and Zackai,G. (1989) *J. Mol. Biol.*, **210**, 829–848.
Rothschild,K.J., Braiman,M.S., Mogi,T., Stern,L.J. and Khorana,H.G. (1989) *FEBS Lett.*, **250**, 448–452.
Siebert,F. (1991) In Dürr,H. and Bouas-Laurent,H. (eds), *Studies in Organic Chemistry, Photochromic Materials: Theory and Application*. Elsevier, in press.
Smith,S.O., Hornung,I., van der Steen,R., Pardoen,J.A., Braiman,M.S., Lugtenburg,J. and Mathies,R.A. (1986) *Proc. Natl Acad. Sci. USA*, **83**, 967–971.
Smith,S.O., Pardoen,J.A., Lugtenburg,J. and Mathies,R.A. (1987) *J. Phys. Chem.*, **91**, 804–819.
Soppa,J. and Oesterhelt,D. (1989) *J. Biol. Chem.*, **264**, 13043–13048.
Soppa,J., Ottomo,J., Straub,J., Tittor,J., Meessen,S. and Oesterhelt,D. (1989) *J. Biol. Chem.*, **264**, 13049–13056.
van der Steen,R., Biesheuvel,P.L., Mathies,R.A. and Lugtenburg,J. (1986) *J. Amer. Chem. Soc.*, **108**, 6410–6411.
Stockburger,M., Alshuth,T., Oesterhelt,D. and Gärtner,W. (1986) In Clark,R.J.H. and Hester,R.E. (eds), *Advances in Spectroscopy*. J. Wiley and Sons, London, Vol. 13, pp. 483–535.
Trissl,H.W. and Gärtner,W. (1987) *Biochemistry*, **26**, 751–758.
Tsygannik,I.N. and Baldwin,J.M. (1987) *Eur. Biophys. J.*, **14**, 263–272.
Wagner,G., Hartmann,R. and Oesterhelt,D. (1978) *Eur. J. Biochem.*, **89**, 169–179.

Received on October 8, 1990; revised on May 27, 1991